Pathol. Oncol. Res. (2014) 20:335–341
DOI 10.1007/s12253-013-9700-7

RESEARCH

In-Vitro and In-Vivo Imaging of Prostate Tumor Using $NaYF_4$: Yb, Er Up-Converting Nanoparticles

Yongjiang Yu · Tao Huang · Yu Wu · Xiaorong Ma · Guopeng Yu · Jun Qi

Received: 7 May 2013 / Accepted: 2 October 2013 / Published online: 14 November 2013

Abstract The aim of this study was to investigate the feasibility of prostate tumor bioimaging both in vitro and in vivo using an upconversion fluorophore, $NaYF_4$: Yb, Er nanoparticles. Luminescent signals of human prostate cancer cells (CWR22R and LNCaP) labeled with $NaYF_4$: Yb, Er nanoparticles were detected by laser scanning confocal microscope, while Cy3 or FITC was used as control probe. Mouse-human prostate cancer model was developed by subcutaneously injecting the CWR22R cells into BALB/c nude mice to investigate the in-vivo imaging properties of $NaYF_4$:Yb, Er nanoparticles. Both CWR22R and LNCaP cells could phagocytose $NaYF_4$:Yb, Er nanoparticles in vitro, and the cellular uptake of CWR22R cells was much higher than that of LNCaP cells (95.42±3.47 % vs. 51.63±6.43 %), which made us choose the former for the further study. CWR22R cells pre-labeled with $NaYF_4$:Yb, Er nanoparticles showed no obvious decrease of fluorescence intensity ($P>0.05$) after light exposure, while the fluorescence intensity of Cy3 or FITC labeled cells decreased rapidly with prolonged bleaching ($P<0.05$). Furthermore, the in-vivo results showed that the prostate cancer cells pre-labeled with or without $NaYF_4$:Yb, Er nanoparticles formed tumors 4 weeks after injection, and the tumor length-diameter of the nanoparticle group and the control group was (10.3±2.0) mm and (9.8±2.5) mm, respectively. Significant upconversion fluorescence signals were observed in the tumors of the nanoparticle group when being excited at 980 nm by a NIR laser. In summary, the results suggest that as an intensive fluorescence imaging label agent, $NaYF_4$:Yb, Er nanoparticles possess unique features and can be used for imaging prostate tumor cells both in vitro and in vivo by phagocytosis.

Keywords $NaYF_4$:Yb, Er · Nanoparticles · Prostate tumor cells · Biological imaging

Y. Yu · T. Huang · Y. Wu · G. Yu · J. Qi (✉)
Department of Urology, Xinhua Hospital, Shanghai Jiaotong University School of Medicine, No.1665 Kongjiang Road, Yangpu District, Shanghai 200092, China
e-mail: jasonqi@sh163.net

X. Ma
Department of Plastic Surgery, Xinhua Hospital, Shanghai Jiaotong University School of Medicine, Shanghai 200092, China

Introduction

Prostate cancer is the most common malignant tumor diagnosed in men and remains the second leading cause of cancer death in western countries [1, 2]. In recent years, clinical incidence of this disease is increasing in significance worldwide [3]. Because of the high incidence and long latent period, early detection of prostate cancer plays a critical role in designing effective therapeutic plans [4].

During the last decades, there has been a rapid development of nanotechnology to diagnose and treat cancer [5, 6]. Some nanoparticles doped with rare-earth activator ions Er^{3+}, Yb^{3+} or Ho^{3+} have recently been synthesized [7]. Rare-earth upconversion nanoparticles (UCNPs) display the unique property of emitting visible light following photo-excitation with near-infrared laser light [8]. Compared with other conventional fluorescent probes based on single-photon excitation, UCNPs possess some important features as fluorescent probes in biological labeling and imaging technology: the absence of background fluorescence in biological tissues, the remarkable light penetration depth and much improved photochemical stability [9–11]. These nanoparticles have recently been used as luminescent labels for bioimaging [12, 13]. Further development of UCNPs, such as direct immunolabeling, in situ hybridization and incorporation into microspheres will offer many opportunities in various research fields across chemistry, biology and medicine.

Rare-earth UCNPs are typically composed of two types of dopant ions to guarantee the luminescence efficiency, an activator and a donator [14]. The activator usually emits visible light while the donator is an energy sensitizer. Yb^{3+}, which has high absorption coefficient and upconversion efficiency, is usually selected as the sensitizer [15]. Er^{3+}, Tm^{3+}, and Ho^{3+} are good choices for activators, which enable efficient energy transfer from Yb3+ to them [16]. Yb/Er co-doped $NaYF_4$ nanoparticles are known as one of the most efficient NIR-to-visible upconverting phosphors [17]. A number of studies have reported that $NaYF_4$:Yb, Er nanoparticles can be used in cellular and tissue imaging sensitively [18, 19]. It is hopeful that $NaYF_4$:Yb, Er can be used for clinical tumor biological research as well.

In this work, we try to find out whether $NaYF_4$:Yb, Er nanoparticles can be taken up by human prostate cancer cells and exhibit special advantages as photo luminescent probes of bioimaging.

Materials and Methods

Experimental Reagents and Instruments

F12, Fetal Bovine Serum (FBS), L-glutamine, mycillin and Trypsin-EDTA was purchased from GIBICO, mouse anti human prostate-specific membrane antigen (PSMA) monoclonal antibodies was purchased from Abcam, anti-mouse IgG-Cy3 secondary antibody and anti-mouse IgG-FITC secondary antibody were obtained from Jackson Immune Research. All other chemicals were of analytical reagent grade and used without further purification. BALB/c nude mice (5–6 weeks of age) were purchased from Slack laboratory animals LLC (Production license number. SYXK (Hu) 2007–0005, Xinhua hospital laboratory animal certificate of fitness number: 2003–0031). Animal studies were performed in compliance with guidelines set by China Ethics Committee and ethical standards. $NaYF_4$:Yb, Er nanoparticles was gifted by professor Li Fuyou from Department of Chemistry of Fudan University.

Inverted phase contrast microscope (Olympus), laser scanning confocal microscope (Olympus) with 980 nm stimulator (NIR), in-vivo living image system (Kodak) fitted with adjustable continuous near infrared stimulator and DU897 EMCCD signal receiver were used to detect images of the samples.

Culture of Cancer Cells

Human prostate cancer cells (HPCCs) (CWR22R and LNCaP) were cultured in F12 culture medium supplemented with 10 % FBS, 1 % L-glutamine and 1 % mycillin at a temperature of 37 °C in an environment containing 5 % CO_2.

In Vitro Culture of HPCC with $NaYF_4$:Yb,Er Nanoparticles

HPCCs (CWR22R and LNCaP) were incubated with 30 μg/ml $NaYF_4$:Yb, Er for 24 h, washed three times with PBS, and fixed with 4 % paraformaldehyde solution for 20 min. After a slight washing with PBS, the cells were sealed with distilled water. Finally, the samples were excited by Laser scanning confocal microscope at 980 nm, and the luminescent signals were detected in two channels: green channel (500–560 nm) and red channel (600–700 nm). Afterwards, the sealed samples were exposed to nature light for 2 h and the fluorescence intensity was tested at intervals. The results were also recorded by laser scanning confocal microscope and the color value of the images was calculated by Flviewer-1000 software.

PSMA Immunofluorescence Labeling of HPCC

CWR22R cells near confluence were washed with phosphate buffer solution (PBS), then fixed with 4 % paraformaldehyde for 20 min, and followed by another washing in PBS 3 times, 5 min each. Bovine Serum Albumin (BSA, 3 %) was added to block non-specific antigen on the cell surface. Anti PSMA monoclonal antibodies (1 : 100) were added to the samples. All the samples were then cultured at 4 °C overnight, washed thrice with PBS 5 min each, and incubated with FITC/Cy3-secondary antibody at room temperature for 2 h with a subsequent washing. DAPI nucleic stain was performed by adding DAPI to the samples at room temperature for 5 min. Finally, the samples were sealed with distilled water. Images were taken by laser scanning confocal microscope before and after exposure to nature light for 2 h for bleaching, and the color value of the images was calculated by Flviewer-1000 software.

Development of Tumor Mouse Model Using HPCC (CWR22R) Cultured with $NaYF_4$:Yb, Er Nanoparticles and its Fluorescence Image

CWR22R Cells incubated with 30 μg/ml $NaYF_4$:Yb, Er nanoparticles for 24 h were trypsinized and removed to 10 ml centrifuge tubes. The cells were harvested by centrifugation at a low-speed (1,000×g) for 5 min, and then diluted with culture medium to a density of 10×10^6 cells/ml. Thirty two BALB/c nude mice (male and female), aged 5–6 weeks, were randomly divided into two groups ($n=16$). The nanoparticle group was subcutaneously injected with 0.2 ml CWR22R cell suspension (2×10^6 cells) labeled with $NaYF_4$:Yb, Er nanoparticles into their left back sites to establish tumor models, while no-label CWR22R cells were used in the control group instead. We then took the in-vivo images of the anesthetized mice and monitored the tumor length (8–10 mm) for 4 weeks.

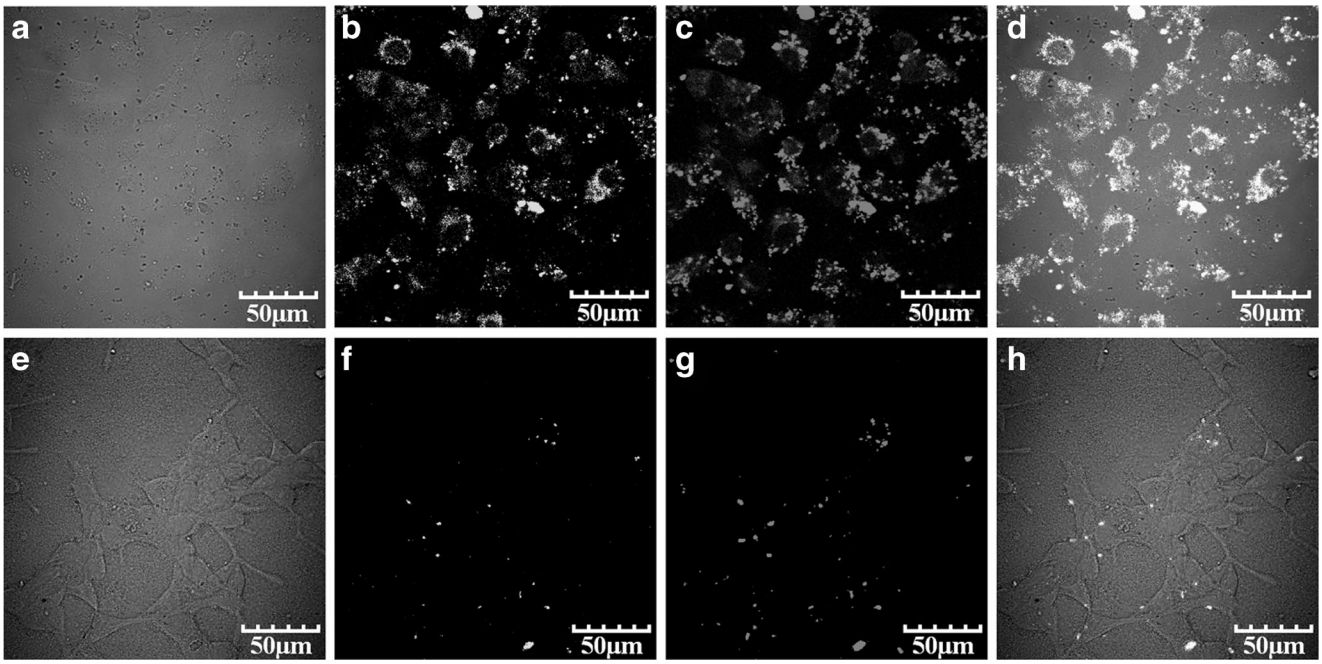

Fig. 1 Fluorescence images of CWR22R and LNCaP cells. **a**–**d** CWR22R cells incubated with $NaYF_4$:Yb, Er nanoparticles; **e**–**f** LNCaP cells incubated with $NaYF_4$:Yb, Er nanoparticles. A, E: Phase contrast microscope; **b**, **f** Emission light at wavelength between 500 and 560 nm; **c**, **g** Emission light at wavelength between 600 and 700 nm; **d** Merge of **a** to **c**; **h** Merge of **e** to **g**

Statistical Methods

SAS 6.12 software package was used for analysis, and data were expressed as mean ± standard deviation. Furthermore, comparison between two groups was performed by *t*-test. $P<0.05$ was considered statistically significant.

Results

$NaYF_4$:Yb, Er Nanoparticles Uptake by HPCCs

Cellular uptake of $NaYF_4$:Yb, Er nanoparticles by two different prostate cancer cells (CWR22R and LNCaP) was detected

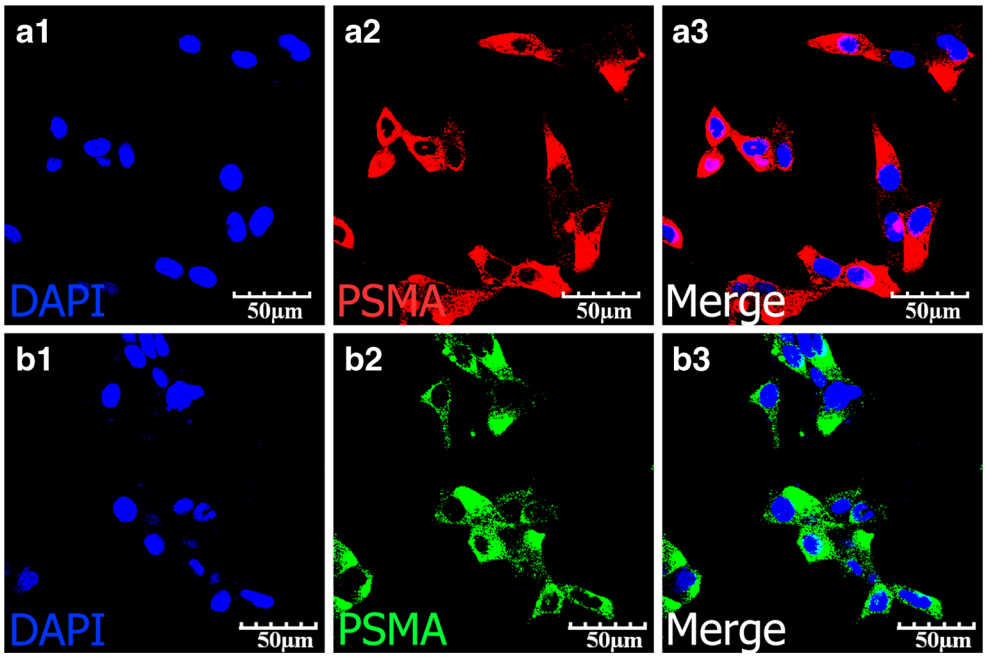

Fig. 2 Immunofluorescence staining of PSMA on CWR22R cells. **a** Cy3-coniugated anti mouse IgG antibody was served as secondary antibody; **b** FITC-conjugated anti mouse IgG antibody was served as secondary antibody. The nuclei were counterstained with DAPI. (× 600, Bar=50 μm)

quantificationally. As shown in Fig. 1, a significantly higher uptake of nanoparticles was observed in CWR22R cell line (P <0.05): 95.42±3.47 % of CWR22R cells can phagocytose $NaYF_4$:Yb, Er nanoparticles (Fig. 1a), while only 51.63± 6.43 % of LNCaP cells can phagocytose the same nanoparticles (Fig. 1b).

PSMA Immunofluorescence Labeled CWR22R Cells

Fixed CWR22R cells were firstly incubated with a mouse anti-PSMA antibody, followed by an anti-mouse IgG-Cy3/ FTIC secondary antibody. As shown in Fig. 2, both anti-mouse IgG-Cy3 secondary antibody and anti-mouse IgG-FITC secondary antibody bound to the monoclonal antibody successfully and produced corresponding fluorescence signals after excitation. From the two merging images (Fig. 2A3 and B3), the observed fluorescence from the separate stains was coincident throughout the cells.

Comparison of Fluorescence Intensity Among $NaYF_4$:Yb, Er Nanoparticles, Cy3 and FITC in CWR22R Cells

The nanoparticles were exposed to nature light at the same excitation light and observed at intervals by Laser scanning

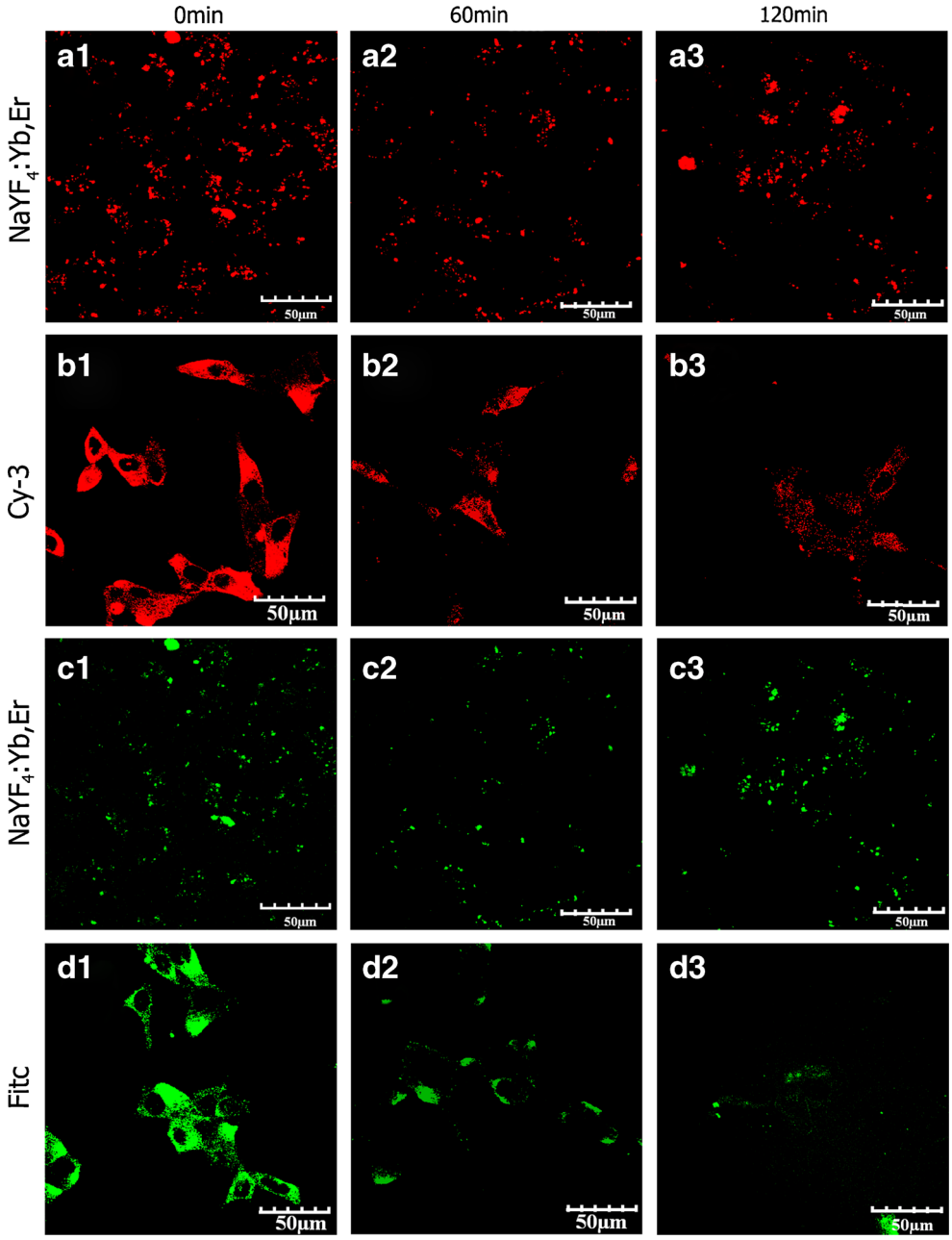

Fig. 3 Fluorescence quenching of NaYF4:Yb, Er, Cy3 and FITC labeled on CWR22R cells after photobleaching. **a** Fluorescence quenching of NaYF4:Yb, Er, emission light 600–700 nm; **b** Fluorescence quenching of Cy3; **c** Fluorescence quenching of NaYF4:Yb, Er, emission light 500–560 nm; **d** Fluorescence quenching of FITC

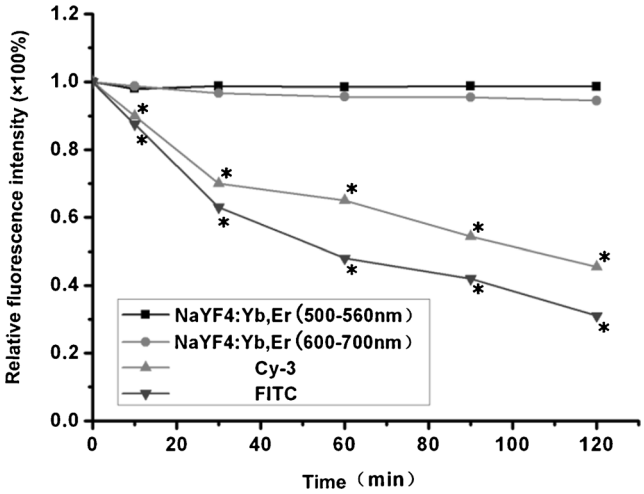

Fig. 4 Fluorescence intensity of NaYF4:Yb, Er, Cy3 and FITC labeled on CWR22R cells after photobleaching from 0 to 120 min, * $P<0.05$ vs. pre-photobleaching

confocal microscope in green channel (500–560 nm) and red channel (600–700 nm). In general, $NaYF_4$:Yb, Er nanoparticles showed strong resistance to photo-bleaching. The fluorescence intensity of the nanoparticles phagocytosed by CWR22R cells was not reduced at all after bleaching: the green and red fluorescence intensity was 98.60±8.66 % and 94.53±5.18 %, respectively ($P>0.05$, Figs. 3a, c and 4). In contrast, the fluorescence intensity of Cy3 and FITC reduced significantly after 2 h nature light bleaching, measured as 45.52±5.31 % and 31.15±3.66 %, respectively ($P<0.05$, Figs. 3b, d and 4).

The Biological Images of $NaYF_4$:Yb, Er Nanoparticles in Mouse-Human Prostate Cancer Model

The efficacy of $NaYF_4$:Yb, Er nanoparticles as luminescence labels for fluorescence in vivo in BALB/c nude mice was investigated further. Three mice in the nanoparticle group and four in the control group formed subcutaneous prostate tumor in the fourth week, and the length-diameter of the tumors was 10.3±2.0 mm and 9.8±2.5 mm, respectively. Anaesthetized mice were then imaged using Kodak in vivo imaging system in which excitation was provided by laser scanning confocal microscope at 980 nm and upconversion luminescence signals were collected by DU897 EMCCD. As shown in Fig. 5, a significant upconversion luminescence signal was observed in the tumor of the nanoparticle group, whereas no significant luminescence signal was observed in the tumor of the control group. The successful in-vivo tumor imaging indicated that $NaYF_4$:Yb, Er nanoparticles could be phagocytosed by CWR22R cells and produce strong upconversion fluorescence when being excited at 980 nm by a NIR laser. The study also suggests that $NaYF_4$:Yb, Er nanoparticles can potentially be used for bioimaging.

Discussion

Immunofluorescence is a very important technique for detecting biological and clinical tissues, protein and antigen expression of organisms [20, 21]. Conventional fluorescence imaging techniques, including organic dyes [22, 23] and semiconductor quantum dots [24] have some intrinsic

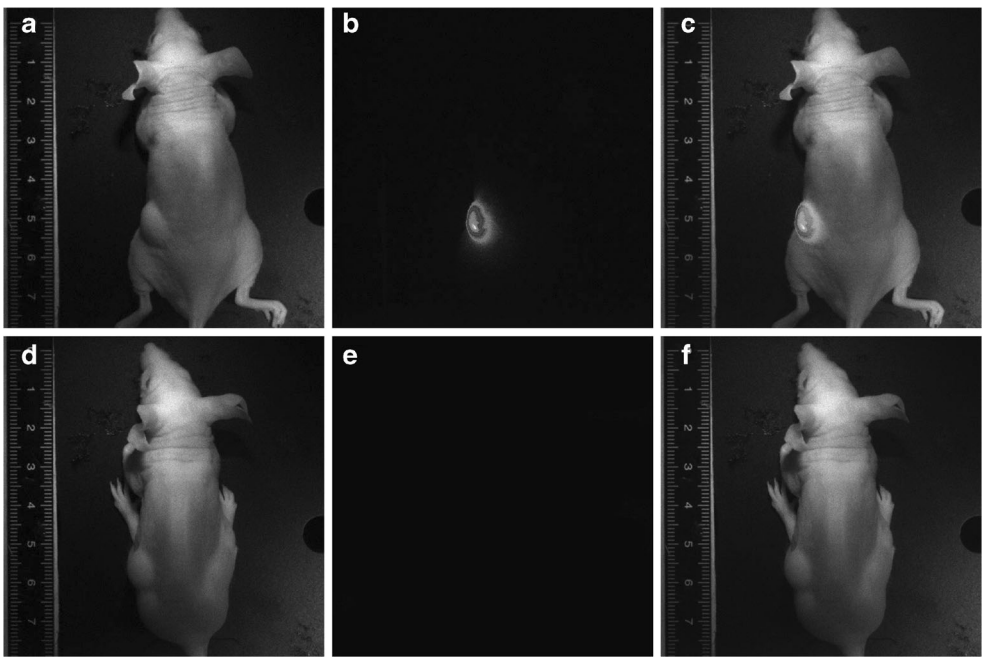

Fig. 5 In-vivo biological imaging of NaYF4:Yb, Er nanoparticles in human prostate cancer model in mice. **a** Optical photo of the nanoparticle group mice; **b** In-vivo biological imaging of NaYF4:Yb, Er nanoparticles in human prostate cancer model in mice under NIR excitation; **c** Merge of **a**–**b**; **d** Optical photo of the control group mice; **e** In-vivo biological imaging of the control group mice; **f** Merge of **d**–**e**

limitations, such as photobleaching, high background autofluorescence and short penetration depth in biological tissues [25]. Recently, the emergence of a new and promising biological luminescent label through the use of rare-earth upconversion nanoparticles has attracted a tremendous amount of attention [26, 27]. The unique properties of these upconversion nanoparticles, such as long lifetimes, superior photostability and sharp absorption and emission lines [28], allow for their use as direct probes or sensitizers for traditional probes. The potential materials not only provide alternatives for their use as photo luminescent probes but also open up new possibilities for many multicolor experiment and diagnosis [29].

Yb/Er co-doped $NaYF_4$ nanoparticles ($NaYF_4$:Yb, Er) have been reported as one of the most efficient fluorescence materials. The synthesis of this important new class of materials made the assumption of composing a material with a controlled size of less than 100 nm and high bright luminescence ability come true. In this study, both in- vitro and in-vivo imaging of human prostate cancer cells prelabeled with $NaYF_4$ nanoparticles co-doped with lanthanide ions Yb/Er have been investigated.

Two types of prostate cancer cell lines were chosen for our experiments: CWR22R and LNCaP. CWR22R cells are the androgen-independent cell line which were obtained by selecting tumors for regrowth and increased serum PSA after androgen withdrawal. Some investigations using CWR22R cell line to develop in-vivo models have been reported in recent years [30, 31]. LNCaP cells are the androgen-dependent cell line of human prostate cancer most commonly used in prostate cancer researches.

It was found in our study that after incubated with 30 μg/ml of $NaYF_4$:Yb, Er nanoparticles for 24 h, both CWR22R and LNCaP cells can phagocytose $NaYF_4$:Yb, Er nanoparticles and develop in-vitro imaging of living cells. Under 980 nm laser excitation, the two different kinds of cells labeled by $NaYF_4$:Yb, Er nanoparticles can both exhibit bright green or red fluorescence. Nevertheless, the nanoparticle uptake of CWR22R cells is higher than LNCaP under the same experimental condition, which may be caused by the difference of their phagocytosis ability. Thus, CWR22R cells were chosen for the further study. Tumors were generated by transplanting the CWR22R cells incubated with 30 μg/ml of $NaYF_4$:Yb, Er nanoparticles for 24 h in vitro to nude mice. Phagocytosed $NaYF_4$:Yb, Er nanoparticles were at the tumor site after 4 weeks and showed excellent fluorescence imaging effect. The results of this study suggest a new tracer method for biological researches of tumor cells in animal such as tumor cell metastasis.

Photo stability is the most important characteristic of fluorescence medium. However, the traditional organic dyes are easy to quench after bleaching [32–34]. Our results showed that the fluorescence intensity of Cy3 and FITC decreased to 45.52±5.31 % and 31.15±3.66 % respectively after 2 h of natural light bleaching, which will directly cause the failure of researches and diagnosis when they are used as tracers of animal or human tumor cell metastasis. The green and red fluorescence intensity of $NaYF_4$:Yb, Er nanoparticles remained 98.60±8.66 % and 94.53±5.18 % respectively after bleaching for 2 h with natural light. It didn't quench obviously because of its unique physicochemical properties, showing incomparable photo stability in fluorescence imaging.

Conclusions

In summary, we reported the applications of upconversion fluorescence nanoparticles $NaYF_4$:Yb, Er for in-vitro imaging of HPCCs and in-vivo imaging in tumor-bearing animals. As an imaging medium which has strong fluorescence intensity, $NaYF_4$:Yb, Er nanoparticles can not only label and image tumor cells through phagocytosis, but also have significant photo stability, being a potential fluorescence label both in human tumor imaging and diagnosis.

Conflict of Interest All authors have no conflict of interest.

Disclosure of Grants or Other Funding None.

References

1. Ren J, Wang F, Wei G, Yang Y, Liu Y, Wei M, Huan Y, Larson AC, Zhang Z (2012) MRl of prostate cancer antigen expression for diagnosis and immunotherapy. PLoS One 7(6):e38350. doi:10.1371/journal.pone.0038350
2. Jemal A, Siegel R, Xu J, Ward E (2010) Cancer statistics, 2010. CA Cancer J Clin 60(5):277–300. doi:10.3322/caac.20073caac.20073
3. Haas GP, Delongchamps N, Brawley OW, Wang CY, de la Roza G (2008) The worldwide epidemiology of prostate cancer: perspectives from autopsy studies. Can J Urol 15(1):3866–3871
4. Abdolahi M, Shahbazi-Gahrouei D, Laurent S, Sermeus C, Firozian F, Allen BJ, Boutry S, Muller RN (2013) Synthesis and in vitro evaluation of MR molecular imaging probes using J591 mAb-conjugated SPIONs for specific detection of prostate cancer. Contrast Media Mol Imaging 8(2):175–184. doi:10.1002/cmmi.1514
5. Ferrari M (2005) Cancer nanotechnology: opportunities and challenges. Nat Rev Cancer 5(3):161–171. doi:10.1038/nrc1566
6. Peer D, Karp JM, Hong S, Farokhzad OC, Margalit R, Langer R (2007) Nanocarriers as an emerging platform for cancer therapy. Nat Nanotechnol 2(12):751–760. doi:10.1038/nnano.2007.387
7. He F, Yang P, Wang D, Li C, Niu N, Gai S, Zhang M (2011) Preparation and up-conversion luminescence of hollow La2O3:Ln (Ln = Yb/Er, Yb/Ho) microspheres. Langmuir 27(9):5616–5623. doi:10.1021/la200506q
8. Chatterjee DK, Rufaihah AJ, Zhang Y (2008) Upconversion fluorescence imaging of cells and small animals using lanthanide doped nanocrystals. Biomaterials 29(7):937–943. doi:10.1016/j.biomaterials.2007.10.051

9. Idris NM, Li Z, Ye L, Sim EK, Mahendran R, Ho PC, Zhang Y (2009) Tracking transplanted cells in live animal using upconversion fluorescent nanoparticles. Biomaterials 30(28):5104–5113. doi:10.1016/j.biomaterials.2009.05.062
10. Yu M, Li F, Chen Z, Hu H, Zhan C, Yang H, Huang C (2009) Laser scanning up-conversion luminescence microscopy for imaging cells labeled with rare-earth nanophosphors. Anal Chem 81(3):930–935. doi:10.1021/ac802072d10.1021/ac802072d
11. Xiong L, Chen Z, Tian Q, Cao T, Xu C, Li F (2009) High contrast upconversion luminescence targeted imaging in vivo using peptide-labeled nanophosphors. Anal Chem 81(21):8687–8694. doi:10.1021/ac901960d
12. Wang C, Tao H, Cheng L, Liu Z (2011) Near-infrared light induced in vivo photodynamic therapy of cancer based on upconversion nanoparticles. Biomaterials 32(26):6145–6154. doi:10.1016/j.biomaterials.2011.05.007
13. Mader HS, Kele P, Saleh SM, Wolfbeis OS (2010) Upconverting luminescent nanoparticles for use in bioconjugation and bioimaging. Curr Opin Chem Biol 14(5):582–596. doi:10.1016/j.cbpa.2010.08.014
14. Lin M, Zhao Y, Wang S, Liu M, Duan Z, Chen Y, Li F, Xu F, Lu T (2012) Recent advances in synthesis and surface modification of lanthanide-doped upconversion nanoparticles for biomedical applications. Biotechnol Adv 30(6):1551–1561. doi:10.1016/j.biotechadv.2012.04.009
15. Soukka T, Rantanen T, Kuningas K (2008) Photon upconversion in homogeneous fluorescence-based bioanalytical assays. Ann N Y Acad Sci 1130:188–200. doi:10.1196/annals.1430.0271130/1/188
16. Wang F, Liu X (2009) Recent advances in the chemistry of lanthanide-doped upconversion nanocrystals. Chem Soc Rev 38(4):976–989. doi:10.1039/b809132n
17. Lim SF, Ryu WS, Austin RH (2010) Particle size dependence of the dynamic photophysical properties of NaYF4:Yb, Er nanocrystals. Opt Express 18(3):2309–2316. doi:10.1364/OE.18.002309195128
18. Cao T, Yang T, Gao Y, Yang Y, Hu H, Li F (2010) Water-soluble NaYF ₄: Yb/Er upconversion nanophosphors: synthesis, characteristics and application in bioimaging. Inorg Chem Commun 13(3):392–394
19. Wang M, Mi CC, Wang WX, Liu CH, Wu YF, Xu ZR, Mao CB, Xu SK (2009) Immunolabeling and NIR-excited fluorescent imaging of HeLa cells by using NaYF(4):Yb, Er upconversion nanoparticles. ACS Nano 3(6):1580–1586. doi:10.1021/nn900491j
20. Egerer K, Roggenbuck D, Hiemann R, Weyer MG, Buttner T, Radau B, Krause R, Lehmann B, Feist E, Burmester GR (2010) Automated evaluation of autoantibodies on human epithelial-2 cells as an approach to standardize cell-based immunofluorescence tests. Arthritis Res Ther 12(2):R40. doi:10.1186/ar2949ar2949
21. Chan KH, Kwan JS, Ho PW, Ho JW, Chu AC, Ramsden DB (2010) Aquaporin-4 autoantibodies in neuromyelitis optica spectrum disorders: comparison between tissue-based and cell-based indirect immunofluorescence assays. J Neuroinflammation 7:50. doi:10.1186/1742-2094-7-501742-2094-7-50
22. Xiong L, Yu M, Cheng M, Zhang M, Zhang X, Xu C, Li F (2009) A photostable fluorescent probe for targeted imaging of tumour cells possessing integrin alpha(v)beta(3). Mol Biosyst 5(3):241–243. doi:10.1039/b820576k
23. Yu M, Zhao Q, Shi L, Li F, Zhou Z, Yang H, Yi T, Huang C (2008) Cationic iridium(III) complexes for phosphorescence staining in the cytoplasm of living cells. Chem Commun (Camb) 18:2115–2117. doi:10.1039/b800939b
24. Smith AM, Duan H, Mohs AM, Nie S (2008) Bioconjugated quantum dots for in vivo molecular and cellular imaging. Adv Drug Deliv Rev 60(11):1226–1240. doi:10.1016/j.addr.2008.03.015
25. Xiong LQ, Chen ZG, Yu MX, Li FY, Liu C, Huang CH (2009) Synthesis, characterization, and in vivo targeted imaging of amine-functionalized rare-earth up-converting nanophosphors. Biomaterials 30(29):5592–5600. doi:10.1016/j.biomaterials.2009.06.015
26. Lim SF, Riehn R, Ryu WS, Khanarian N, Tung CK, Tank D, Austin RH (2006) In vivo and scanning electron microscopy imaging of up-converting nanophosphors in Caenorhabditis elegans. Nano Lett 6(2):169–174. doi:10.1021/nl0519175
27. Zhang P, Rogelj S, Nguyen K, Wheeler D (2006) Design of a highly sensitive and specific nucleotide sensor based on photon upconverting particles. J Am Chem Soc 128(38):12410–12411. doi:10.1021/ja0644024
28. Chen Z, Chen H, Hu H, Yu M, Li F, Zhang Q, Zhou Z, Yi T, Huang C (2008) Versatile synthesis strategy for carboxylic acid-functionalized upconverting nanophosphors as biological labels. J Am Chem Soc 130(10):3023–3029. doi:10.1021/ja076151k
29. Bruchez M Jr, Moronne M, Gin P, Weiss S, Alivisatos AP (1998) Semiconductor nanocrystals as fluorescent biological labels. Science 281(5385):2013–2016
30. Wu X, Gong S, Roy-Burman P, Lee P, Culig Z (2013) Current mouse and cell models in prostate cancer research. Endocr Relat Cancer. doi:10.1530/ERC-12-0285
31. Bocci G, Di Paolo A, Danesi R (2013) The pharmacological bases of the antiangiogenic activity of paclitaxel. Angiogenesis. doi:10.1007/s10456-013-9334-0
32. Wang HZ, Wang HY, Liang RQ, Ruan KC (2004) Detection of tumor marker CA125 in ovarian carcinoma using quantum dots. Acta Biochim Biophys Sin (Shanghai) 36(10):681–686
33. Wu X, Liu H, Liu J, Haley KN, Treadway JA, Larson JP, Ge N, Peale F, Bruchez MP (2003) Immunofluorescent labeling of cancer marker Her2 and other cellular targets with semiconductor quantum dots. Nat Biotechnol 21(1):41–46. doi:10.1038/nbt764nbt764
34. Ness JM, Akhtar RS, Latham CB, Roth KA (2003) Combined tyramide signal amplification and quantum dots for sensitive and photostable immunofluorescence detection. J Histochem Cytochem 51(8):981–987